

# Open Research Online

The Open University's repository of research publications and other research outputs

## Bioprinting Using Mechanically Robust Core-Shell Cell-Laden Hydrogel Strands

### Journal Item

#### How to cite:

Mistry, Pritesh; Aied, Ahmed; Alexander, Morgan; Shakesheff, Kevin; Bennett, Andrew and Yang, Jing (2017). Bioprinting Using Mechanically Robust Core-Shell Cell-Laden Hydrogel Strands. *Macromolecular Bioscience*, 17(6), article no. 1600472.

For guidance on citations see [FAQs](#).

© 2017 WILEY-VCH Verlag GmbH Co. KGaA, Weinheim



<https://creativecommons.org/licenses/by-nc-nd/4.0/>

Version: Proof

Link(s) to article on publisher's website:  
<http://dx.doi.org/doi:10.1002/mabi.201600472>

Copyright and Moral Rights for the articles on this site are retained by the individual authors and/or other copyright owners. For more information on Open Research Online's data [policy](#) on reuse of materials please consult the policies page.

[oro.open.ac.uk](http://oro.open.ac.uk)



Postfach 10 11 61  
69451 Weinheim  
Germany

*Courier services:*  
Boschstraße 12  
69469 Weinheim  
Germany

Tel.: (+49) 6201 606 581

Fax: (+49) 6201 606 510

E-mail: [macromol@wiley-vch.de](mailto:macromol@wiley-vch.de)

WILEY-VCH

Dear Author,

**Please correct your galley proofs carefully and return them no more than four days after the page proofs have been received.**

The editors reserve the right to publish your article without your corrections if the proofs do not arrive in time.

Note that the author is liable for damages arising from incorrect statements, including misprints.

Please note any queries that require your attention. These are indicated with a Q in the PDF and a question at the end of the document.

**Please limit corrections to errors already in the text; cost incurred for any further changes or additions will be charged to the author, unless such changes have been agreed upon by the editor.**

**Reprints** may be ordered by filling out the accompanying form.

Return the reprint order form by fax or by e-mail with the corrected proofs, to Wiley-VCH : [macromol@wiley-vch.de](mailto:macromol@wiley-vch.de)

To avoid commonly occurring errors, please ensure that the following important items are correct in your proofs (please note that once your article is published online, no further corrections can be made):

- **Names** of all authors present and spelled correctly
- **Titles** of authors correct (Prof. or Dr. only: please note, Prof. Dr. is not used in the journals)
- **Addresses** and **postcodes** correct
- **E-mail address** of corresponding author correct (current email address)
- **Funding bodies** included and grant numbers accurate
- **Title** of article OK
- All **figures** included
- **Equations** correct (symbols and sub/superscripts)

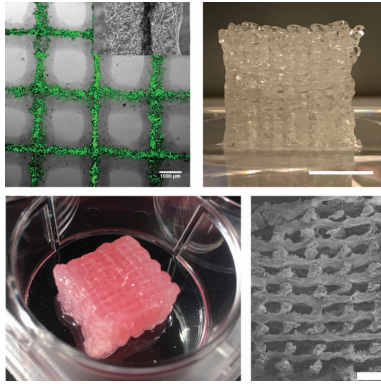
**Corrections should be made directly in the PDF file using the PDF annotation tools. If you have questions about this, please contact the editorial office. The corrected PDF and any accompanying files should be uploaded to the journal's Editorial Manager site.**

Communication

**Bioprinting Using Mechanically  
Robust Core–Shell Cell-Laden  
Hydrogel Strands**

P. Mistry, A. Aied, M. Alexander,  
K. Shakesheff, A. Bennett, J. Yang\*

*Macromol. Biosci.* **2017**, *17*, 1600472



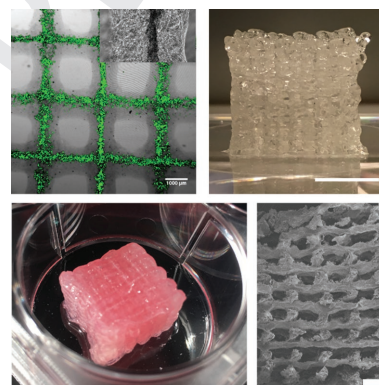
**Combining good biological and mechanical properties in bioprinted constructs** is desirable for them to be employed in many tissue engineering and regenerative medicine applications. Bioprinted cell-laden constructs with core–shell strands have been developed. The cell-supporting materials in the core support high cell viability and tissue-like functions while the shell material offers mechanical robustness to the bioprinted constructs.

UNCORRECTED PROOF

# Bioprinting Using Mechanically Robust Core–Shell Cell-Laden Hydrogel Strands

Pritesh Mistry, Ahmed Aied, Morgan Alexander, Kevin Shakesheff, Andrew Bennett, Jing Yang\*

The strand material in extrusion-based bioprinting determines the microenvironments of the embedded cells and the initial mechanical properties of the constructs. One unmet challenge is the combination of optimal biological and mechanical properties in bioprinted constructs. Here, a novel bioprinting method that utilizes core–shell cell-laden strands with a mechanically robust shell and an extracellular matrix-like core has been developed. Cells encapsulated in the strands demonstrate high cell viability and tissue-like functions during cultivation. This process of bioprinting using core–shell strands with optimal biochemical and biomechanical properties represents a new strategy for fabricating functional human tissues and organs.



## 1. Introduction

The development of highly organized and functional 3D tissue constructs remains an unmet challenge. Bioprinting is emerging as a promising technology for recapitulating 3D hierarchical tissue/organ structures comprising multiple cell types and extracellular matrix (ECM). For bioprinted constructs to survive and function during in vitro

maturation, particularly where mechanical stimulation is applied, and after implantation, both the biological and mechanical properties of bioprinted tissue constructs are critical. Hydrogels that are widely used to encapsulate cells in bioprinting, therefore, are required to offer tailored biological and mechanical properties to support the survival and functions of encapsulated cells and maintain the initial structural integrity of the 3D constructs. Despite significant advances in bioprinting of tissues and organs, the combination of optimal biological and mechanical properties in bioprinted cell-laden hydrogel constructs has not been achieved. In this paper, we describe a novel extrusion-based bioprinting process that utilizes core–shell cell-laden strands with a mechanically robust hybrid hydrogel shell and an ECM-mimicking hydrogel core. The ECM-mimicking hydrogels, such as collagen and Matrigel, supported high cell viability and in vivo like cell functions, meanwhile the hybrid hydrogel shell supplied mechanical robustness, such as shape recovery after compression. Three different cell types were encapsulated in bioprinted structures consisting of core–shell strands, all of which displayed high cell viability during culture. A vascular-like morphology from the human umbilical vein endothelial cells (HUVECs) and albumin secretion by HepG2 cells in the core were demonstrated. The release rates of two proteins from the strands were found to

**Mr** P. Mistry, **Dr** A. Aied, **Prof** K. Shakesheff,  
**Dr** J. Yang  
Division of Drug Delivery and Tissue Engineering  
School of Pharmacy  
University of Nottingham  
Nottingham NG7 2RD, UK  
E-mail: jing.yang@nottingham.ac.uk  
**Prof** M. Alexander  
Division of Surface Analysis and Biophysics  
School of Pharmacy  
University of Nottingham  
Nottingham NG7 2RD, UK  
**Dr** A. Bennett  
FRAME Laboratory  
School of Life Sciences  
University of Nottingham  
Nottingham NG7 2RD, UK

correlate with the rate of swelling. These core-shell strands can be used to fabricate hierarchical tissue constructs with desirable biological and mechanical properties.

Since the early work in which a microfluidic device was used to make continuous solid and hollow fibers,<sup>[1]</sup> a body of work has been published on cell-laden hydrogel fibers/strands with different configurations (solid, hollow, and core-shell configurations) formed by using microfluidic devices<sup>[1–7]</sup> as well as extrusion through coaxial needles.<sup>[8–12]</sup> To form 3D structures, bioprinting utilizing coaxial needles has been used to fabricate structures with solid,<sup>[7,13]</sup> hollow strands,<sup>[10,11]</sup> and core-shell strands.<sup>[14,15]</sup> However, the materials used in the coaxial bioprinting have not been optimized for optimal cell viability/function and mechanical robustness of the printed constructs. Alginate has been used in these bioprinting processes due to its rapid gelation when encountering multivalent cations. However, alginate lacks cell-binding sites for supporting cell spreading,<sup>[16]</sup> which resulted in suboptimal cell viability and function in these bioprinted constructs with cell-laden solid or hollow strands. To create an ECM-like microenvironment for encapsulated cells, core-shell fibers with an ECM protein core and an alginate shell have been shown to support the long-term culture of encapsulated cells; these cells exhibited tissue-like morphologies and functions.<sup>[6]</sup> A purpose-built microfluidic weaving machine was used to assemble these core-shell fibers into higher-order structures.<sup>[6]</sup> However, the ability to fabricate complex 3D geometries using the textile manufacturing technology is limited. Moreover, alginate hydrogels are relatively brittle and lack flexibility for in vitro manipulation and implantation. The strategy of combining hydrogels has been found to markedly improve the mechanical properties.<sup>[17–19]</sup> However, those hydrogels were made using harsh conditions which inhibited the encapsulation of cells. Recently, a hybrid hydrogel prepared under cell-compatible conditions has been used to encapsulate cells, and subsequently it has been 3D printed into various cellular 3D geometries.<sup>[18]</sup> While improved toughness and the ability to recover its shape after compression were achieved, the hybrid hydrogel lacked the biological properties for optimal cell survival and function. Despite these significant advances in bioprinting using cell-laden strands, one remaining challenge is the bioprinting of tissue-relevant architectures using strands with combined optimal biological and mechanical properties. Here we have developed a novel bioprinting method that utilizes core-shell cell-laden strands, which have a mechanically robust shell and an ECM-like core to achieve both optimal biological and mechanical properties.

In our approach, the core-shell strands were bioprinted using a coaxial needle mounted onto a commercial 3D printer (Figure 1A,B). Bioprinting using a coaxial needle was chosen because the core and the shell materials

formed a composite strand which combined the cell-supporting and the mechanical properties of the core and the shell, respectively. The central nozzle was perfused with a cell-laden hydrogel, while the outer nozzle was perfused with a partially crosslinked alginate or a hybrid hydrogel comprising alginate and poly(ethylene glycol) diacrylate (PEGDA). The partial crosslinking gave alginate and the hybrid gel solutions a suitable viscosity range (Figure 1C) for the formation of a continuous strand during the extrusion-based bioprinting process (Movie S1, Supporting Information).  $17 \times 10^{-3}$  M calcium chloride was found to generate a viscosity range that is suitable for the printing of both alginate and hybrid gels. Addition of PEGDA to alginate resulted in an increase in viscosity. However, both the partially crosslinked alginate and hybrid gels showed similar viscosities (Figure 1C), which suggests that the viscosity of the printable gels was mainly determined by the crosslinking caused by calcium ions. The partial crosslinking of the alginate shell eliminated the need to use highly concentrated alginate<sup>[10]</sup> to achieve a suitable viscosity for printing, as well as the requirement to co-perfuse highly concentrated calcium chloride in the core to form alginate strands.<sup>[7,11,13]</sup> The core-shell configuration also allowed for the inclusion of cell-laden collagen and Matrigel, which are usually too fluidic for shape fixation via the extrusion-based bioprinting method. The core-shell configuration of the printed strands was well defined with the cellular core positioning approximately in the center of the strands (Figure 1D). Cell-laden strands were printed into thick multilayered constructs that would not be possible to fabricate using textile manufacturing methods (Figure 1E,F). We noticed that the partially crosslinked hydrogels were relatively soft, which consequently compromised the interconnectivity of pores during printing. This was due to the sinking of strands that were printed above a layer where the gaps between the two supporting strands were wide. Therefore, a coprinting method was developed in which gelatine strands were printed in the gaps between the core-shell strands for supporting, and subsequently removed by incubating in cell culture medium at 37 °C (Movie S2, Supporting Information). A 20-layered construct was made using this method (Figure 1E). By immersing the coprinted constructs in a calcium chloride solution and subsequently in culture medium at 37 °C, gelatine was removed efficiently and the shape was maintained (Figure 1F). Imaging the cross section (side view of the constructs) using scanning electron microscopy (SEM) after the removal of gelatine showed that the pores were open and interconnected (Figure 1G).

When a hybrid gel (PEGDA/alginate) was used as the shell material, each layer of a multilayer construct was crosslinked using UV before the next layer was printed on top in order to ensure the uniform crosslinking of PEGDA. Repeated UV exposure during the printing of thick



49 Q3



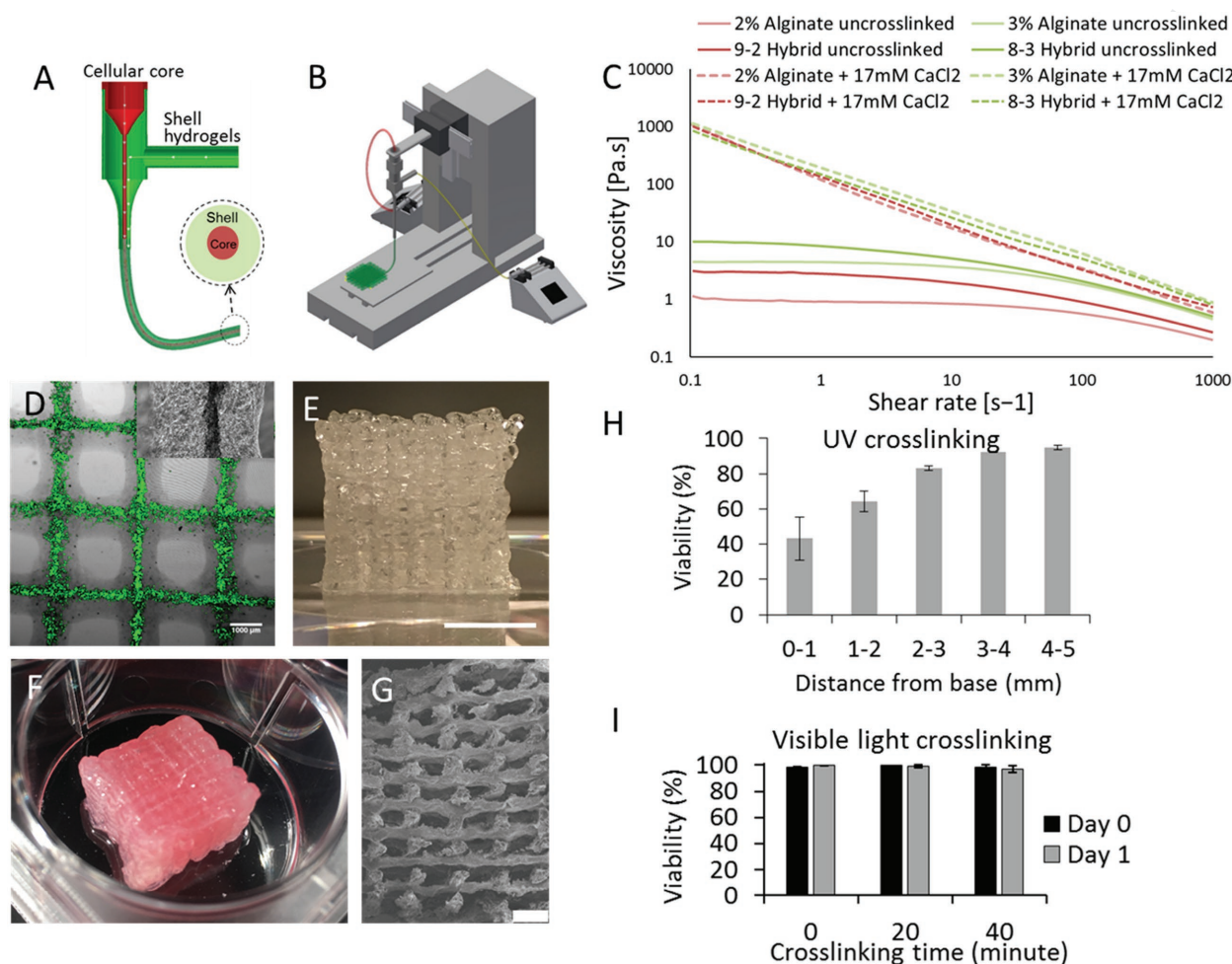


**Figure 1.** 3D bioprinting using core–shell cell-laden strands. A,B) Schematic diagram depicting the coaxial needle and the printer assembly. C) Viscosities of uncrosslinked and partially crosslinked alginate and hybrid gels. D) A 3D printed lattice comprised of core–shell (hybrid gel) strands with fluorescently labelled cells in the core surrounded by the shell (darker gray). The inset is a bright-field image showing the core and shell. Scale bar: 1 mm. E) A bioprinted 20-layer construct using coprinting of cell-laden core–shell (hybrid gel) strands and gelatine strands. Scale bar: 10 mm. F) A printed construct after removal of gelatine showing structural integrity. G) SEM image of the cross section (side profile) of a bioprinted construct showing interconnected pores after the removal of gelatine. Scale bar: 1 mm. H) Viability of 3T3 fibroblasts in a six-layer construct with 1 min UV exposure for each layer. The construct was manually cut into five layers from base to top for viability evaluation. I) Viability of 3T3 fibroblasts after exposure to visible light for different time periods. Error bars represent standard deviation,  $n = 3$ .

constructs was found to lower cell viability, which was caused by the penetration of UV light into lower layers during crosslinking of the top layer (Figure 1H). We therefore replaced the UV-activated photoinitiator (Irgacure 2959) with a visible-light-activated photoinitiator (lithium phenyl-2,4,6-trimethyl-benzoylphosphine (LAP)).<sup>[20,21]</sup> Cells encapsulated in the visible-light-crosslinked methacrylated gelatine (GelMA) showed high viability, even after long exposure to the light (Figure 1I). Tall Cell-laden constructs could therefore be printed without compromising the viability of cells (Movie S3, Supporting Information). Although the strand diameter (ca. 800  $\mu\text{m}$ ) was greater than those made using microfluidic devices (ca. 200  $\mu\text{m}$ ), high cell viability was maintained during

culturing (Figure 2), suggesting that transportation of nutrients and oxygen was sufficient through the shell to the cellular core.

To investigate cell survival, morphology, and function within the bioprinted structures constructed from core–shell strands, three different cell types were separately encapsulated in three different core materials. The combinations of cell type and core hydrogel (gelatine methacrylate, collagen, Matrigel) is shown in Figure 2A. High cell viability were maintained during the culture period of 28 d. 3T3 fibroblast culture was terminated at day 7 due to the rapid proliferation and consequent confluence of cells. The cell viabilities between constructs with alginate or the hybrid gel (9:2, PEGDA: alginate

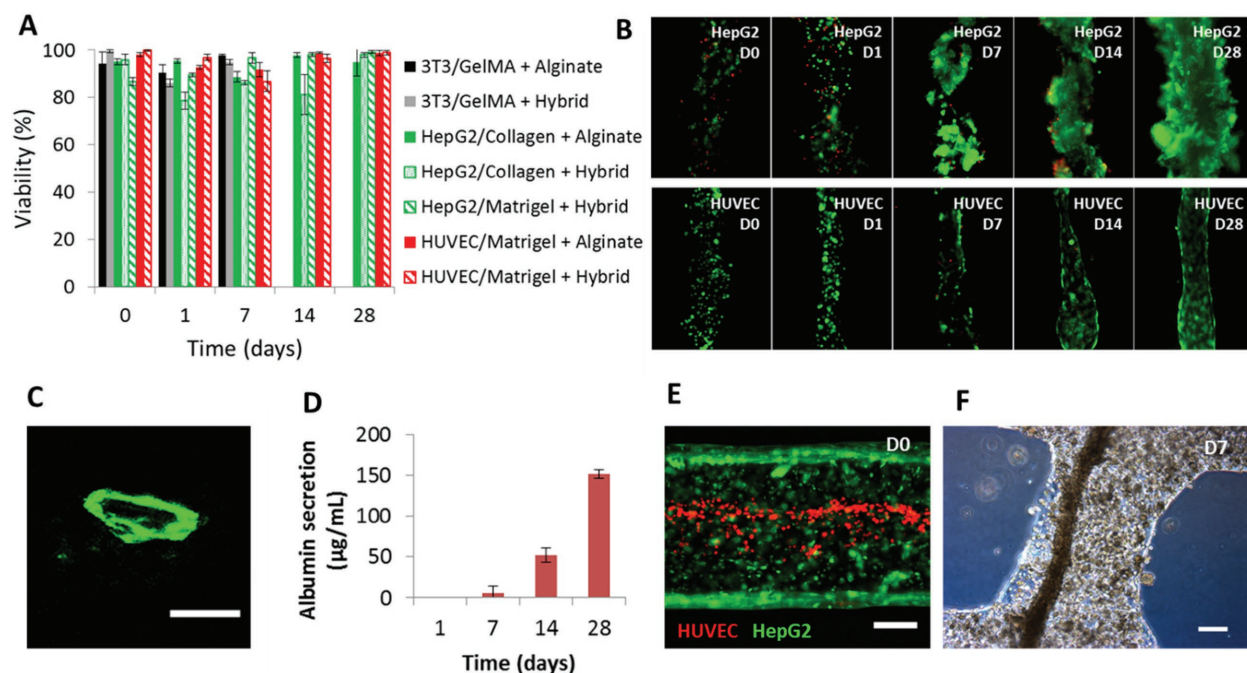


**Figure 2.** Cell viability, morphology, and function within bioprinted constructs with core-shell strands. **A)** Viability of three different cell types in the core-shell strands with different core and shell materials. **B)** Cell morphologies in the cores of core-shell strands during 28 d of culturing. Cells were labelled using green-fluorescent calcein-AM (live cells) and red-fluorescent ethidium homodimer-1 (dead cells). **C)** Formation of a vascular-like structure from bioprinted HUVECs in a transversely cut core-shell strand at day 44. Scale bar = 100 µm. **D)** Albumin secretion of HepG2 cells in bioprinted constructs. **E,F)** Bioprinted HUVECs and HepG2 cells in the core and shell respectively at day 0 and day 7. The cells were fluorescently labelled at day 0 using a red and a green cell tracker, respectively. Scale bar: 200 µm. Error bars represent standard deviation,  $n = 3$ .

(%) shell were similar. Immediately after printing, the HUVECs appeared discrete and rounded, and were a mixture of individual cells and cell aggregates. The HUVECs began to spread in the Matrigel core by day 1, and had organized themselves to form a vascular-like structure by day 7. This vascular-like structure was maintained from day 7 to day 28. HUVECs were cultured up to 44 d, and showed high cell viability (Figure S1, Supporting Information). On day 44 of the HUVEC culture, the strands were cut transversely to image the cross sections. The formation of a vascular-like structure within the strands was observed (Figure 2C). It appeared that the vascular-like channels were formed at the boundary between the core and the shell (Figure S1, Supporting Information), suggesting that it is possible to control the diameter of the channel by varying the size of the central needle. The embedded HepG2 cells exhibited an increase in albumin secretion over time (Figure 2D), which correlated with the increase in cell numbers as evidenced in Figure 2B.

We have also demonstrated that two different cell types can be coprinted into the core and shell, respectively. Figure 2E shows the bioprinted strands with hepatocytes in the alginate shell and HUVECs in the Matrigel core. After 7 d of cultivation, the HUVECs in the core formed a vascular-like structure, similar to that formed in the strands with an acellular shell (Figure 2F). HepG2

cells in the alginate shell formed multiple cell aggregates. Although the channels formed by the HUVECs are larger than liver sinusoids, this bioprinted multicellular structure is representative of the natural arrangement of endothelial cells and hepatocytes in liver. The capability of including two cell types in the core and shell, respectively, suggests the possibility of fabricating vascularized mini-tissues using these core-shell strands. The cell type in the shell can potentially be changed, implying that these core-shell strands can be used to fabricate different vascularized mini tissues.

Next, we measured the tensile properties of alginate/PEGDA hybrid gels with different compositions. Three hybrid gel compositions (namely 10:1, 9:2, and 8:3, PEGDA:alginate (%)) were examined while the overall hybrid gel concentration was fixed at 11% (w/v). The tensile properties of these materials were assessed using molded dumbbell-shaped samples, and are shown in Figure 3A. Representative stress-strain curves are shown in Figure S2 in the Supporting Information. The modulus and ultimate tensile strength (UTS) of the hybrid gels increased with the concentration of alginate. The strengths of the hybrids were much higher than the sums of the individual components, suggesting a synergistic effect (Figure S3, Supporting Information). This synergistic effect is likely due to the entanglement of alginate



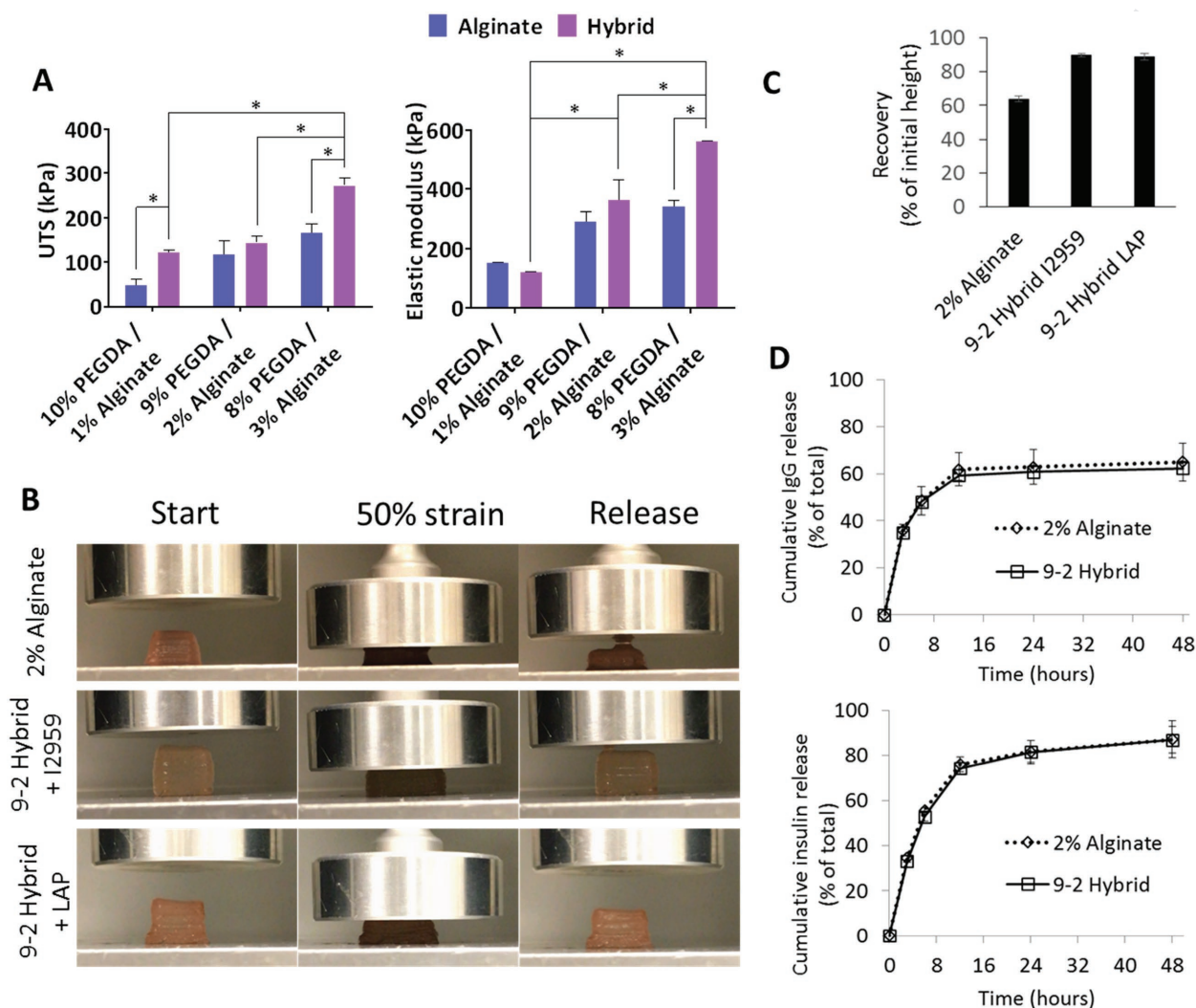


**Figure 3.** Mechanical properties and protein release properties of bioprinted constructs. A) Tensile properties of dumbbell-shaped hydrogels. B) Shape changes of bioprinted ten-layered solid constructs with cell-laden core–shell strands after compression to 50% strain. C) Quantified shape recovery using the percentage of initial height after compression. D) Human IgG and human insulin release profiles from printed constructs with core–shell strands. Error bars represent standard deviation,  $n = 3$ . The \* sign denotes statistical difference using  $\alpha = 0.05$ .

and PEGDA chains; chain entanglement in hydrogels is a contributor to their mechanical properties.<sup>[22]</sup> The 9:2 and 8:3 hybrid gels showed an increase in all three mechanical properties (modulus, UTS, and failure strain) compared to pure alginate gels, with a maximum 65% increase in UTS for the 8:3 hybrid gels (Table S1, Supporting Information). Up to 3% alginate was used in our study. While higher concentrations can further increase the modulus and strength of gels, they can also reduce the transportation of nutrients<sup>[23–25]</sup> and cell viability.<sup>[26,27]</sup> Both PEGDA and alginate have been tested in clinical trials and have shown good biocompatibility.<sup>[28,29]</sup> In this study, we have used calcium chloride to replace the low-solubility calcium sulfate used in previous studies,<sup>[18]</sup> eliminating the presence of solid calcium sulfate particles in the final printed constructs. Though calcium sulfate was shown to be biocompatible

as a bone substitute in animal testing,<sup>[30]</sup> its presence may not be desirable in other applications. Bioprinted solid constructs with cell-laden core–shell strands were assessed using compression testing. The constructs were compressed to 50% of their original height and then released immediately. The printed constructs with the hybrid gel (9:2, PEGDA:alginate (%)) showed significantly more shape recovery compared to pure alginate counterparts.

The degradation of the core and shell materials used in our study has been previously reported. The core materials (collagen I, Matrigel, GelMA) are likely to degrade faster than the shell materials (PEGDA and alginate) due to enzymatic degradation of these protein-based materials.<sup>[31–33]</sup> The degradation of PEGDA has been attributed to the hydrolysis of the esters rather than the backbone ethers.<sup>[34]</sup> The modulus of PEGDA, which was implanted



in a rat, showed progressive reduction at an average rate of 6% per week. Degradation of alginate relies on the gradual exchange of calcium, which crosslinks guluronic acid blocks, for monovalent cations.<sup>[35]</sup> Oxidation can also be used to make alginate degradable under physiological conditions.<sup>[36]</sup> The difference in degradation rates means that the remodeling processes in the core and the shell, respectively, are different. The shell material would remain longer than the core material after implantation, which is beneficial for maintaining structural stability.

These core-shell strands can potentially be used for immunoprotective roles to encapsulate allogenic cells or for delivering therapeutic proteins. To test the release of proteins from the strands, two proteins of different sizes were studied: human insulin (6.6 kDa) and human IgG (150 kDa). Figure 3D shows the release profiles of proteins from the bioprinted constructs with core-shell strands. The results show no significant differences between the hybrid shell and the pure alginate shell, suggesting that the addition of crosslinked PEGDA does not reduce the overall mesh size significantly, with regard to the sizes of the investigated proteins. The cumulative release of insulin is greater than that of IgG, suggesting that higher-molecular-weight proteins are more likely to be entrapped within the gels. The times at which the protein releases started to plateau were similar to the time (11 h) at which the swelling reached maximum (Figure S4, Supporting Information), suggesting the rapid release may be related to the increase of hydrogel mesh size caused by swelling. The rate of protein release agrees with previous observations made on protein release from alginate beads.<sup>[37,38]</sup>

In summary, we have bioprinted 3D structures with core-shell strands that have a mechanically robust shell and an ECM-mimicking core. Interconnected pores were introduced by using a coprinting process. Bioprinting using the core-shell hydrogel strands allows more complex 3D geometries to be formed compared to textile manufacturing methods. Compared to previous coaxial bioprinting, the materials we employed enhanced the mechanical robustness of the constructs, and the survival and function of encapsulated cells. Separately encapsulated, three cell types in the core showed high viability within bioprinted constructs consisting of core-shell strands. The formation of a tissue-like morphology by the HUVECs was also observed. In addition, we were able to coprint endothelial cells in the core and HepG2 cells in the shell to fabricate mini tissues with vascular-like structures, which can potentially be assembled to form larger and more complex tissues using bioprinting. By adding PEGDA to alginate, the hybrid gels showed greater tensile moduli and strengths compared to pure alginate. The shape recovery after compression was also significantly improved by using hybrid gel strands. The rates of protein diffusion through the alginate and hybrid gel

shell showed no difference. This process of bioprinting using core-shell strands with combined biochemical and biomechanical properties represents a new strategy for fabricating functional human tissues and organs.

## 2. Experimental Section

### 2.1. 3D Bioprinting with Core-Shell Strands

Constructs with core-shell strands were printed using a coaxial needle (27G/18G inner and outer needles, respectively) mounted onto a commercial 3D bioprinter (RegenHU, Switzerland). The core and shell were driven by two separate syringe pumps using flow rates of 0.01 and 0.1 mL min<sup>-1</sup>, respectively. Hydrogel solutions for the shell were prepared by dissolving either PEGDA (20 kDa; Sigma-Aldrich) or alginate (FMC Biopolymer) individually, or in combination, in deionized water at the desired (w/v) concentrations. For the hybrid hydrogels, the total hydrogel concentration was fixed at 11% (w/v). Iracure 2959 (I2959; Sigma-Aldrich) or LAP (TCI Chemicals) was added as the photoinitiator at a final concentration of 0.1% or 0.13% (w/v), respectively, in the hybrid gel solutions. The shell hydrogel solutions were partially crosslinked by mixing with calcium chloride solutions to reach a final concentration of  $17 \times 10^{-3}$  M calcium ions. For strands with the LAP photoinitiator, visible light (Schott KL1500 LCD) was shone continuously during printing; for strands with the I2959 photoinitiator, UV (power: 15 W;  $\lambda$ : 365 nm; working distance: 35 mm; UVP Cambridge, UK) was shone for 1 min per layer during printing. These constructs were then immersed in a calcium containing buffer ( $100 \times 10^{-3}$  M CaCl<sub>2</sub>,  $150 \times 10^{-3}$  M NaCl,  $25 \times 10^{-3}$  M HEPES, phenol red indicator, deionized water, pH 7.5) for 10 min. The core materials of collagen (Corning) and Matrigel (BD Bioscience) were printed at 5 °C to prevent crosslinking in the cartridge. Type I rat tail tendon collagen was used at a concentration of 3 mg mL<sup>-1</sup>. GelMA was prepared as described previously,<sup>[39]</sup> and 5% (w/v) GelMA in culture medium was used. Four million cells per milliliter were used as the cell density in all cores. 6% (w/v) gelatine was used in the coprinting process.

### 2.2. Formation of Dumbbell-Shaped Hydrogel Samples

All gels were cast in a dumbbell-shaped PTFE mold. The samples had a thickness of 3 mm and a length of 10 mm for the reduced section. If PEGDA was included, the hydrogel solutions were first cured with UV for 2 min before the crosslinking of alginate in a CaCl<sub>2</sub> solution ( $100 \times 10^{-3}$  M) for 10 min. Pure alginate hydrogels were prepared by first pre-crosslinking with a CaSO<sub>4</sub> slurry at a fixed alginate:CaSO<sub>4</sub> ratio of 1:0.1328. The solution was immediately cast into the mold and left for 5 min with a glass slide to cover the top. The pure alginate hydrogels were then immersed in a  $100 \times 10^{-3}$  M CaCl<sub>2</sub> bath for 10 min.

### 2.3. Tensile and Compression Testing of Hydrogels

The tensile properties the hydrogels were measured at room temperature using a Universal Texture Analyser (TA-HD Plus,

Stable Microsystems, USA). The grip section of each dumbbell-shaped gel was wrapped with paper towel to improve gripping. A constant deformation speed of  $0.5 \text{ mm s}^{-1}$  was applied during the test. The tests were stopped after the samples broke. Compression testing was carried out using the same machine on bioprinted solid constructs ( $8 \times 8 \times 8 \text{ mm}^3$ , ten layers) with cell-laden core–shell strands.

## 2.4. Cell Culture

All cells were cultured at  $37^\circ\text{C}$  with 5%  $\text{CO}_2$ . HepG2 cells (ATCC) were used up to passage 20, and were cultured in Eagle's minimal essential medium (Sigma-Aldrich) supplemented with 9% (v/v) fetal bovine serum (FBS; Sigma-Aldrich),  $2 \times 10^{-3} \text{ M}$  L-glutamine (Sigma-Aldrich), 1% nonessential amino acids (Gibco), and 1% antibiotic/antimycotic (Sigma-Aldrich). The 3T3 mouse fibroblast (3T3) cells (ATCC) were used up to passage 65, and were cultured in DMEM supplemented with 9% FBS,  $2 \times 10^{-3} \text{ M}$  L-glutamine, and 1% antibiotic/antimycotic. Primary HUVECs (PromoCell) were used up to passage 6, and were cultured in endothelial cell basal medium (PromoCell).

## 2.5. Cell Viability and Albumin Secretion

Cell viability was measured using a live/dead kit (ThermoFisher, UK). To measure cell viability in LAP crosslinked GelMA, one million cells per milliliter of 3T3 fibroblasts were encapsulated in 5% (w/v) GelMA containing 0.13% (w/v) LAP. Light (working distance: 25 mm) was shone on the gels for different time periods, after which culture media was added.

Fluorescent images were taken using a fluorescence microscope (Leica). The albumin secretion was measured using an ELISA kit (Abcam, UK) and a plate reader (Infinite M200, Tecan).

## 2.6. Protein Release Studies

Lattice constructs ( $20 \times 20 \times 1.6 \text{ mm}^3$ , two layers) were printed with a core of GelMA (5%) loaded with either recombinant human insulin (Sigma-Aldrich) or recombinant human IgG (Sigma-Aldrich). The concentrations of insulin and IgG in the cores were 174 and  $10 \mu\text{g mL}^{-1}$  respectively. Constructs were incubated in culture medium at  $37^\circ\text{C}$ . At regular intervals, the medium was taken and replaced with fresh medium. ELISA was used to examine the medium samples for the presence of insulin (Simple-Step Human Insulin ELISA; Abcam) or IgG by (Human IgG ELISA; Sigma-Aldrich).

## 2.7. Statistical Analysis

One-way ANOVA with Tukey's posthoc test was used for statistical analysis. An  $\alpha$  value of 0.05 was used in both methods.

## Supporting Information

Supporting Information is available from the Wiley Online Library or from the author.

**Acknowledgements:** The authors would like to thank EPSRC and MRC Centre for Doctoral Training in Regenerative Medicine for sponsoring Pritesh Mistry's studentship.

Received: November 9, 2016; Published online: ; DOI: 10.1002/mabi.201600472

**Keywords:** bioprinting; hydrogels; mechanical properties; tissue engineering

- W. Jeong, J. Kim, S. Kim, S. Lee, G. Mensing, D. J. Beebe, *Lab Chip* **2004**, *4*, 576.
- S. Shin, J.-Y. Park, J.-Y. Lee, H. Park, Y.-D. Park, K.-B. Lee, C.-M. Whang, S.-H. Lee, *Langmuir* **2007**, *23*, 9104.
- K. H. Lee, S. J. Shin, Y. Park, S.-H. Lee, *Small* **2009**, *5*, 1264.
- M. Yamada, S. Sugaya, Y. Naganuma, M. Seki, *Soft Matter* **2012**, *8*, 3122.
- E. Kang, G. S. Jeong, Y. Y. Choi, K. H. Lee, A. Khademhosseini, S.-H. Lee, *Nat. Mater.* **2011**, *10*, 877.
- H. Onoe, T. Okitsu, A. Itou, M. Kato-Negishi, R. Gojo, D. Kiriya, K. Sato, S. Miura, S. Iwanaga, K. Kuribayashi-Shigetomi, Y. T. Matsunaga, Y. Shimoyama, S. Takeuchi, *Nat. Mater.* **2013**, *12*, 584.
- C. Colosi, S. R. Shin, V. Manoharan, S. Massa, M. Costantini, A. Barbetta, M. R. Dokmeci, M. Dentini, A. Khademhosseini, *Adv. Mater.* **2016**, *28*, 677.
- R. A. Perez, M. Kim, T.-H. Kim, J.-H. Kim, J. H. Lee, J.-H. Park, J. C. Knowles, H.-W. Kim, *Tissue Eng., Part A* **2014**, *20*, 103.
- J. O. Buitrago, R. A. Perez, A. El-Fiqi, R. K. Singh, J.-H. Kim, H.-W. Kim, *Acta Biomater.* **2015**, *28*, 183.
- Y. Luo, A. Lode, M. Gelinsky, *Adv. Healthcare Mater.* **2013**, *2*, 777.
- Q. Gao, Y. He, J.-Z. Fu, A. Liu, L. Ma, *Biomaterials* **2015**, *61*, 203.
- Y. Zhang, Y. Yu, A. Akkouch, A. Dababneh, F. Dolati, I. T. Ozbolat, *Biomater. Sci.* **2015**, *3*, 134.
- C. Colosi, M. Costantini, R. Latini, S. Ciccarelli, A. Stampella, A. Barbetta, M. Massimi, L. C. Devirgiliis, M. Dentini, *J. Mater. Chem. B* **2014**, *2*, 6779.
- G. Kim, S. Ahn, Y. Kim, Y. Cho, W. Chun, *J. Mater. Chem.* **2011**, *21*, 6165.
- A. R. Akkineni, T. Ahlfeld, A. Lode, M. Gelinsky, *Biofabrication* **2016**, *8*.
- K. Y. Lee, D. J. Mooney, *Prog. Polym. Sci.* **2012**, *37*, 106.
- J.-Y. Sun, X. Zhao, W. R. K. Illeperuma, O. Chaudhuri, K. H. Oh, D. J. Mooney, J. J. Vlassak, Z. Suo, *Nature* **2012**, *489*, 133.
- S. Hong, D. Sycks, H. F. Chan, S. Lin, G. P. Lopez, F. Guilak, K. W. Leong, X. Zhao, *Adv. Mater.* **2015**, *27*, 4035.
- J. P. Gong, Y. Katsuyama, T. Kurokawa, Y. Osada, *Adv. Mater.* **2003**, *15*, 1155.
- B. D. Fairbanks, M. P. Schwartz, C. N. Bowman, K. S. Anseth, *Biomaterials* **2009**, *30*, 6702.
- T. Majima, W. Schnabel, W. Weber, *Macromol. Chem. Phys.* **1991**, *192*, 2307.
- F. Jiang, T. Huang, C. He, H. R. Brown, H. Wang, *J. Phys. Chem. B* **2013**, *117*, 13679.
- O. Holte, H. H. Tonnesen, J. Karlsen, *Pharmazie* **2006**, *61*, 30.
- L. M. Weber, C. G. Lopez, K. S. Anseth, *J. Biomed. Mater. Res. A* **2009**, *90A*, 720.
- S. Lee, X. Tong, F. Yang, *Acta Biomater.* **2014**, *10*, 4167.
- S. P. M. Bohari, D. W. L. Hukins, L. M. Grover, *Bio-Med. Mater. Eng.* **2011**, *21*, 159.

- [27] J. P. Mazzocchi, D. L. Feke, H. Baskaran, P. N. Pintauro, *J. Biomed. Mater. Res. A* **2010**, *93A*, 558.
- [28] G. Basta, P. Montanucci, G. Luca, C. Boselli, G. Noya, B. Barbaro, M. Qi, K. P. Kinzer, J. Oberholzer, R. Calafiore, *Diabetes Care* **2011**, *34*, 2406.
- [29] B. Sharma, S. Fermanian, M. Gibson, S. Unterman, D. A. Herzka, B. Cascio, J. Coburn, A. Y. Hui, N. Marcus, G. E. Gold, J. H. Elisseeff, *Sci. Transl. Med.* **2013**, *5*.
- [30] M. Nilsson, J. S. Wang, L. Wielanek, K. E. Tanner, L. Lidgren, *J. Bone Jt. Surg., Br. Vol.* **2004**, *86B*, 120.
- [31] C. N. Grover, R. E. Cameron, S. M. Best, *J. Mech. Behav. Biomed. Mater.* **2012**, *10*, 62.
- [32] C. B. Hutson, J. W. Nichol, H. Aubin, H. Bae, S. Yamanlar, S. Al-Haque, S. T. Koshy, A. Khademhosseini, *Tissue Eng., Part A* **2011**, *17*, 1713.
- [33] J. E. Valentin, A. M. Stewart-Akers, T. W. Gilbert, S. F. Badylak, *Tissue Eng., Part A* **2009**, *15*, 1687.
- [34] M. B. Browning, S. N. Cereceres, P. T. Luong, E. M. Cosgriff-Hernandez, *J. Biomed. Mater. Res. A* **2014**, *102*, 4244.
- [35] H. J. Kong, D. Kaigler, K. Kim, D. J. Mooney, *Biomacromolecules* **2004**, *5*, 1720.
- [36] K. H. Bouhadir, K. Y. Lee, E. Alsberg, K. L. Damm, K. W. Anderson, D. J. Mooney, *Biotechnol. Prog.* **2001**, *17*, 945.
- [37] C. J. Gray, J. Dowsett, *Biotechnol. Bioeng.* **1988**, *31*, 607.
- [38] H. Tanaka, M. Matsumura, I. A. Veliky, *Biotechnol. Bioeng.* **1984**, *26*, 53.
- [39] A. I. Van den Bulcke, B. Bogdanov, N. De Rooze, E. H. Schacht, M. Cornelissen, H. Berghmans, *Biomacromolecules* **2000**, *1*, 31.

## Query

- Q1: Please provide the highest academic title (either Dr. or Prof.) for all authors, where applicable.
- Q2: As per style, there should be headings in "Macromolecular" articles. We have added the first heading "Introduction" and numbered the rest headings accordingly. Please check for correctness.
- Q3: Please confirm if 'SEM' is the correct acronym for 'scanning electron microscopy.'
- Q4: Please define 'IgG', 'HEPES', 'PTFE', 'DMEM', 'ELISA', 'ANOVA', and '3T3' at their first occurrence in the text.
- Q5: Please provide the page number in refs. (15, 29), if now available.
- Q6: Please check the journal title in ref. (21) for correctness.



## Reprint Order Form 2017



**Editorial Office:**  
Wiley-VCH Verlag  
Boschstraße 12, 69469 Weinheim  
Germany

Tel.: +49 (0) 6201 – 606 – 581  
Fax: +49 (0) 6201 – 606 – 510  
Email: [macromol@wiley-vch.de](mailto:macromol@wiley-vch.de)

**Short DOI: mabi.**

Please send me and bill me for

no. of **Reprints** via ☐ airmail (+ 25 Euro)  
☐ surface mail

Please send me and bill me for a

☐ **high-resolution PDF file** (330 Euro).

My Email address:

Please note: It is not permitted to present the PDF file on the internet or on company homepages.

### Information regarding VAT

Please note that from German sales tax point of view, the charge for **Reprints, Issues or Posters** is considered as “**supply of goods**” and therefore, in general, such delivery is a subject to German sales tax. However, this regulation has no impact on customers located outside of the European Union. Deliveries to customers outside the Community are automatically tax-exempt. Deliveries within the Community to institutional customers outside of Germany are exempted from the German tax (VAT) only if the customer provides the supplier with his/her VAT number. The VAT number (value added tax identification number) is a tax registration number used in the countries of the European Union to identify corporate entities doing business there. It starts with a country code (e.g. FR for France, GB for Great Britain) and follows by numbers.

VAT no.: \_\_\_\_\_

(Institutes / companies in EU countries only)

Purchase Order No.:

**Delivery address / Invoice address:**

Name of recipient, University, Institute, Street name and  
Street number, Postal Code, Country

---

---

---

---

---

---

**Date and Signature:** \_\_\_\_\_

**Credit Card Payment** (optional) -You will receive an invoice.

**VISA. MasterCard. AMERICAN EXPRESS**

Please use the Credit Card Token Generator located at the website below to create a token for secure payment. The token will be used instead of your credit card number.

### Credit Card Token Generator:

[https://www.wiley-vch.de/editorial\\_production/index.php](https://www.wiley-vch.de/editorial_production/index.php)

Please transfer your token number to the space below.

**Credit Card Token Number**

[illegible]

**Price list for reprints** (The prices include mailing and handling charges. All Wiley-VCH prices are exclusive of VAT)

No. of pages	50 copies	100 copies	Price (in Euro) for orders of			
			150 copies	200 copies	300 copies	500 copies
1-4	345	395	425	445	548	752
5-8	490	573	608	636	784	1077
9-12	640	739	786	824	1016	1396
13-16	780	900	958	1004	1237	1701
17-20	930	1070	1138	1196	1489	2022
for every additional 4 pages	147	169	175	188	231	315

Wiley-VCH Verlag GmbH & Co. KGaA; Location of the Company: Weinheim, Germany;  
Trade Register: Mannheim, HRB 432833, Chairman of the Board: Mark Allin  
General Partner: John Wiley & Sons GmbH, Location: Weinheim, Germany  
Trade Register Mannheim, HRB 432296, Managing Director: Sabine Steinbach

WILEY-VCH